Journal of Marine Research, 62, 565–594, 2004

Using JGOFS *in situ* and ocean color data to compare biogeochemical models and estimate their parameters in the subtropical North Atlantic Ocean

by I. Dadou[1], G. Evans[2] and V. Garçon[1]

ABSTRACT

How well do biogeochemical data sets serve to decide among models and model parameter values? Data at 21N, 31W from the French JGOFS EUMELI cruises and the SeaWiFS ocean color sensor were used to estimate parameters for three very different models of biological nitrogen flux in a water column. The three models are (1) an NPZD (Nutrients, Phytoplankton, Zooplankton and Detritus) model (Oschlies *et al.,* 2000), (2) a seven-component model with two pools of dissolved organic matter and detritus with different remineralization and sinking rates (Dadou *et al.,* 2001) and (3) a model of nutrients and phytoplankton including aggregates (Kriest and Evans, 1999). Parameters of the three models are estimated using the same sets of data within the same one-dimensional physical framework. A combination of local and nonlocal optimization methods is used.

It is not easy to decide among candidate models based on their fit to the data. Parameters that mean the same thing in the three models, like the half-saturation concentration for nitrate uptake, were estimated at not very different values in different models. The model with dissolved organic matter, based on its primary production and sediment flux data time evolutions, seems to exhibit the more reasonable annual behavior. Large seasonal changes in deep nitrate data suggest an unexpected role of lateral advection and may vitiate the 1-D approach even at the EUMELI oligotrophic site. The small number of sediment trap measurements are very powerful for constraining the biological nitrogen. Ocean color data did not add extra constraining power.

1. Introduction

The goal of JGOFS (Joint Global Ocean Flux Study) is to assess more accurately, and understand better, the processes controlling regional-to-global and seasonal-to-interannual fluxes of carbon between the atmosphere, surface ocean and ocean interior and their sensitivity to climate changes (SCOR, 1992). Local JGOFS studies are either intensive studies lasting a few weeks (EUMELI (Morel, 1996), NABE (Ducklow and Harris, 1993)) or short visits at regular intervals for many years (BATS (Steinberg *et al.,* 2001)). Such local studies will be informative about regional scales only if they can serve to improve

1. LEGOS/CNRS/UPS/UMR556, 18 Av. E. Belin, 31401, Toulouse, Cedex 9, France. ***email: isabelle.dadou@cnes.fr***

2. Science Branch, Department of Fisheries and Oceans, P.O. Box 5667, St. John's, Newfoundland, A1C 5X1, Canada.

process models, estimate their parameters, decide among different models or suggest new models (SCOR, 1992; Evans and Garçon, 1997).

This paper studies the interplay between two data sets, one collected by the France-JGOFS EUMELI program at the oligotrophic site in the early 1990's, the other the SeaWiFS chlorophyll data set at the same site, and three 1-D biogeochemical models of varying levels of complexity.

How informative are the data? How well do they constrain our knowledge of the processes? Evans (1999) addressed these questions by studying how well NABE data constrain the parameters of one single 0-D model. Here we will investigate whether the data enable us to decide among three different candidate 1-D models for describing the biological processes relevant for biogeochemistry.

2. Methods

a. Data

During the EUMELI program, four cruises devoted to surface and water column processes were carried out between January 1991 and December 1992. Concentrations of different variables were measured and also some rates of transfer among different forms and time-integrated accumulations (from sediment traps). The EUMELI O-site observations have been made available on the France JGOFS site (http://www.obs-vlfr.fr/jgofs). Additional information can be found in a review paper by Morel (2000) and papers of the special EUMELI section in Deep-Sea Research I, *43,* (8), 1996.

i. In situ concentrations. Nitrate and chlorophyll represent the state variables common to all three models. Particulate nitrogen concentrations are compared with the sum of phytoplankton, zooplankton and detritus concentrations in the NPZD and Oli7 models, and with phytoplankton concentration in the SAM model.

In this area, a deep chlorophyll maximum, up to around 0.5 mgChl/m^3, is well developed all year long and the chlorophyll pattern may well not be the phytoplankton pattern (Claustre and Marty, 1995). The nitrogen-to-chlorophyll ratio of phytoplanktonic assemblages sampled was not determined. Nitrate concentrations were compared with the nutrient compartment of the three models. Ocean upper layers at this site are depleted in nitrate (also in phosphate) with values less than 0.1 mmolN/m^3; the nitracline starts up at 100 m depth. Nitrogen particles were collected by an *in situ* pumping system and represent more small particles (living and nonliving) than large particles. Nitrogen content of small particles is low (less than 1 mmolN/m^3) and decreases with depth. Chlorophyll and nitrate data are available for four cruises and nitrogen-particle data only for three cruises (Pujo-Pay and Raimbault, 1994).

ii. In situ flux. Two kinds of flux data were used: primary production and sediment trap data. Primary production data are available for two cruises. Primary production rates

decrease generally from the surface (around 0.004 $gC/m^3/d$) to 120 m (0.001 $gC/m^3/d$) (Morel *et al.,* 1996). A C/N ratio equal to 7 has been used to convert carbon to nitrogen. For sediment trap data, data from the fixed and drifting moorings are available at 250 m depth (Bory *et al.,* 2001; Raimbault, pers. com.). Due to technical *in situ* problems and representativity of this flux at 250 m depth (current speed higher than 15 cm/s for fixed traps), only 9 data points are kept for this study. Fluxes range from 0.47 to 0.02 $mmolN/m^2/d$, with a mean of around 0.13 $mmolN/m^2/d$. Sediment trap data from the drifting mooring are in nitrogen. Fixed sediment trap data were measured in carbon and have been converted to nitrogen using a C/N ratio of 7.

iii. Ocean color satellite data. Ocean color chlorophyll *a* concentration obtained from the SeaWiFS products (level 3 binned data, 8 days, version 3) generated by the NASA Goddard Space Flight Center (GSFC) Distributed Active Archive Center (DAAC) have been used from September 1997 to June 2000. The data were extracted near the O-site and a spatial mean has been applied to remove mesoscale structures (~100 km; Dadou *et al.,* 1996; Oschlies *et al.,* 2000) that the 1D physical frame does not take into account. SeaWiFS chlorophyll concentrations have a mean value of 0.1 $mgChl/m^3$ with a doubling of the mean value in wintertime. The characteristic depth of satellite ocean color signal penetration is 10% of the euphotic layer depth (André, 1991). In this subtropical area, typical euphotic layer depth is around 100 m, so the SeaWiFS data are considered to measure chlorophyll in the top 10 m of the model. From September 1997 to June 2000, 120 observations of the SeaWiFS chlorophyll concentration near the O-site are available.

b. Models

Despite the large effort and expense of the EUMELI program, the resulting data set is still very sparse in time and space. It will not be very informative, will not lead to a large reduction in uncertainty, unless we can augment it with some simplifying assumptions; namely, that the oligotrophic site represents a large, quiet area little disrupted by lateral incursions of water with different properties, and that it undergoes a roughly repeating annual cycle of production and biomass so that observations from different years all represent a single cycle. We therefore constructed three one-dimensional models of biogeochemical variables driven by steady annual cycles of light and mixing and ran them until their solutions had reached a steady annual cycle.

All state variables of the three models are expressed in units of nitrogen.

i. NPZD. Among common models, this is the simplest that can compute the quantities needed for biogeochemistry. Dissolved inorganic *N*utrients are taken up by *P*hytoplankton, whose population is then grazed down by herbivorous *Z*ooplankton. *P* and *Z* then produce *D*etritus that provide the necessary sinking flux through the water column (Fig. 1a). It has been extensively used for biogeochemical studies at the basin scale (Oschlies and Garçon, 1998, 1999; Oschlies *et al.,* 2000) and also for 1-D studies (e.g., Denman and Peña, 1999).

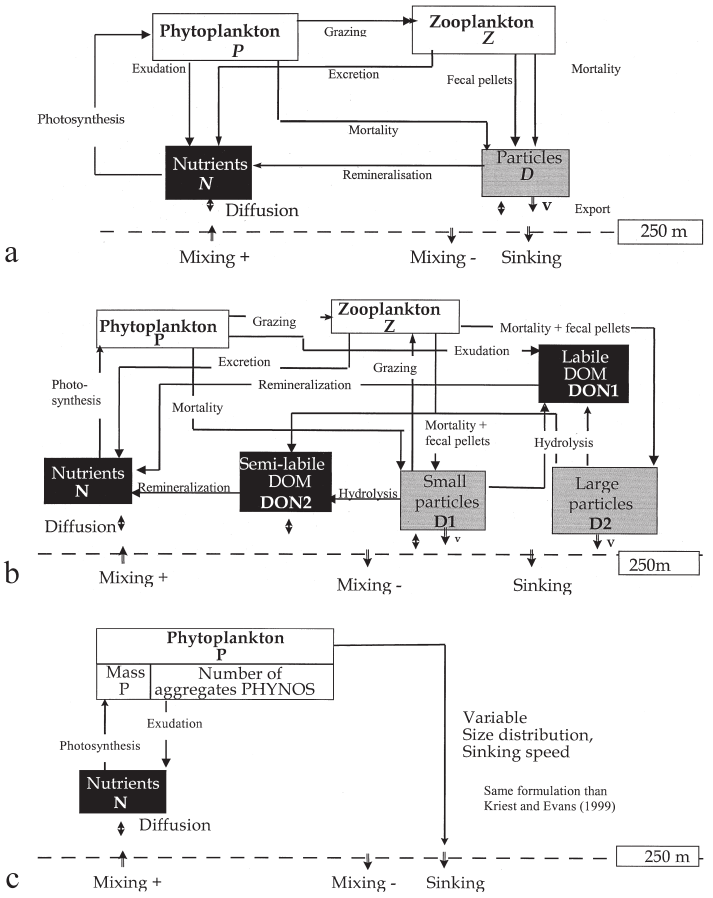

Figure 1. The three biogeochemical model diagrams: (a) NPZD model, (b) Oli7 model and (c) SAM model.

Compared to Oschlies *et al.* (1999, 2000), a fast remineralization loop is taken into account between phytoplankton and nutrients, mimicking a fast remineralization of dissolved organic nitrogen (DON) exuded by phytoplankton. The main limitations of the model are: (1) the dissolved organic matter is not an explicit state variable despite the fact this organic matter seems to play a crucial role in many biogeochemical provinces, (2) the model has only one type of detritus (one size and one sinking speed). The next two models diverge from NPZD in opposite directions.

ii. Oli7. This is a more elaborate model that was designed explicitly to represent the EUMELI *oli*gotrophic site. It incorporates dissolved organic matter, which is considered to be an important reservoir of nitrogen; moreover each of detritus and DON is represented by two classes, to begin to capture the range of possible sinking and regeneration rates. There

are thus *7* state variables (Fig. 1b). The model was designed for coupling with a deep-water model dealing with the necessary complementary processes that turn organic matter back into dissolved nutrients (Dadou *et al.,* 2001).

iii. SAM. The third model takes a direct minimal approach to the question: Why *bio*geochemistry? What does biology have to do with the concentration and flux of trace elements in the ocean? Biology does two main things: it changes chemical compositions to make elements more or less volatile and likely to exchange with the atmosphere, and it makes particles sink through the water rather than only moving with the water. So the model has only dissolved nutrients (N) and phytoplankton particles (mass P and numbers of aggregates); the particles can aggregate and thereby change the speed with which they sink (Fig. 1c). Effectively, the average particle sinking speed becomes a dynamical variable that changes with season and depth. This *S*now *A*ggregation *M*odel was introduced by Kriest and Evans (1999), Kriest (1999), and applied in a more complicated 1-D setting by Kriest and Evans (2000). Its principal characteristic, the ability to produce rapidly sinking flocs following a spring bloom, is perhaps less likely to be displayed at an oligotrophic site with low seasonal variability.

In the three models above, the ratio of cell nitrogen (N) to chlorophyll (Chl) is estimated as a linear function of the amount of light that the cells are adapted to following the formulation of Geider *et al.* (1996, 1997). Typically, the cells are adapted to the light they *see* during a day, so:

$$N/Chl = a_0 + a_1 \cdot \int_{day} I(t)dt$$

with a_0 and a_1 two constants and $I(t)$ the instantaneous light. This formulation affects calculation of phytoplankton growth, attenuation of light by chlorophyll, and the conversion of observed chlorophyll to nitrogen for comparison with model results. The primary production formulation as a function of light and chlorophyll concentration is the formulation of Evans and Parslow (1985) for the three models.

iv. Physical driving. In this study, the 0-dimensional physical frame (Evans, 1999) has been extended to a one-dimensional frame. In the vertical, the 1-D model has 25 levels of 10-meter thickness. The monthly depth of the mixed layer and base of the thermocline has been provided by the study of Dadou *et al.* (2001) using a turbulent kinetic energy model forced with the fluxes of ECMWF daily reanalysis (http://www.ecmwf.int/) at the air-sea interface. The mixed layer thickness changes from 20 m in summer to 100 m in winter. The turbulent vertical eddy diffusion coefficient is set to $k_{\mathrm{ML}} = 100\ \mathrm{cm}^2/\mathrm{s}$ in the mixed layer. Below the base of the thermocline, it is set to a value of $k_{\mathrm{low}} = 1\ \mathrm{cm}^2/\mathrm{s}$. Within the thermocline, it is interpolated using a cubic function presented by Evans and Garçon (1997). A higher background diffusivity below the mixed layer, compared with direct

microstructure measurements (Lewis *et al.,* 1986; Gregg, 1987) and tracer release experiments (Ledwell *et al.,* 1993, 1998), is used in this study as in Doney *et al.* (1996) to take into account additional mixing due to internal waves and occasional eddies advected in the studied area (Morel, 2000; Dadou *et al.,* 1996; Oschlies *et al.,* 2000). The models are driven by day length and daily integrated solar radiation, which has been computed using astronomical formulas (Brock, 1981). Light is reduced by cloudiness following Reed (1976). The three models are run to a steady annual cycle driven by steadily repeating cycles of light and day length as in Evans (1999). The data collected during the EUMELI 1991–1992 cruises are for specific physical dynamical conditions which were different than the climatological average based on the two years 1991–1992. There is no perfect way to deal with this problem (see Evans (1999) for more details). Because mixing and ecological interactions have very different time scales, the model equations are solved using the method of lines and an implicit ordinary differential equation solver (VODE; Brown *et al.,* 1989).

c. Model-data comparisons

The EUMELI oligotrophic site (O-site) (21N, 31W) is situated north of the North Equatorial Current (NEC) in the rather quiet southeastern periphery of the subtropical gyre, though some mesoscale variability associated with the NEC meandering can be expected (Dadou *et al.,* 1996; Oschlies *et al.,* 2000). Therefore, a one-dimensional approach appears reasonable.

For comparing the model predictions with observations, a climatological year was constructed as the different seasons sampled during the EUMELI cruises were for two different years (1991, 1992). SeaWiFS satellite ocean color data since 1997 were also incorporated in this climatological year.

We adjust the model parameters to reduce discrepancies between observations and model predictions. A Box-Cox transformation of the prediction and observation was used (Evans, 2003). So, the misfit function that we minimize has the following form:

$$\sum_{i=1}^{n} 2 \cdot \left(\frac{X_i^{0.5} - x_i^{0.5}}{S^{0.5}} \right)^2 \tag{1}$$

where X_i, x_i are model prediction and corresponding observations, respectively (for the same time and depth). n is the number of single prediction-observation pair (X_i, x_i). Concentrations, rates and time-integrated fluxes with different dimensions are included in the EUMELI biogeochemical data set. S represents the scale factor of the same dimensions as X and x. With this factor, each term of the sum is nondimensional. As the measurement variance is often unknown, we do not choose S to be the standard deviation of the observation error. In this study about biogeochemistry, major concentrations and fluxes of trace elements are the important quantities to get right. We choose to scale by the largest observed value of the variable. The scale factor (S) is equal to $S_{con} = max\,(nitrate\ data)$

for all concentrations, $S_{PP} = (S_{con}/max\ (phytoplankton\ data)) \times max\ (primary\ production)$ for primary production, and $S_{sed} = (S_{con}/max\ (particulate\ nitrogen\ data)) \times max\ (sediment\ trap\ flux\ data)$ for sediment trap fluxes. This choice is explained in detail in Evans (2003). Maximum of phytoplankton data is derived from the maximum chlorophyll concentration data converted to nitrogen using the N/Chl ratio model relationship.

As in Evans (1999), the total misfit function to be minimized is the sum of all the individual model-data (Eq. 1) and parameter-target misfits. The latter misfit is added to the penalty function to penalize deviations from any previous knowledge we might have. If a parameter has a target value P^*, lower and upper bounds P_0 and P_1 and a weight w, then a trial value P is assigned a misfit:

$$w(P - P^*)/(P_1 - P) \quad \text{if } P \geq P^*$$

$$w(P^* - P)/(P - P_0) \quad \text{if } P < P^*.$$

The target parameter values were derived from Oschlies and Garçon (1998), Kriest and Evans (1999) and Dadou *et al.* (2001), or from the EUMELI data like the deep nutrient pool (N_{deep}). The bounds were fixed from the range of values one can find in the literature. For some parameters, like the light attenuation of pure water, tighter bounds have been used as the depth of the euphotic layer has been estimated during the EUMELI cruises. For N_{deep} parameter, the bounds are fixed to the minimum and maximum values derived from the EUMELI O-site data at 250 m depth. In this paper, all weights were chosen equal to 0.1 or less so that the target value had little influence on the total misfit, depending on the confidence we might have on the parameter values. For example, as we know very little about the N/Chl ratio values as a function of light at the O-site, a smaller weight is prescribed for a_0, a_1, and Kc parameters linked to chlorophyll and nitrogen phytoplankton concentration. Sinking speed of particles is also assigned a low weight.

d. Minimizing misfit

Parameter values were estimated by using iterative, derivative-free nonlinear minimization methods to find those parameters that made the misfit function as small as possible. The minimizations were performed with Powell's conjugate direction method (Press *et al.,* 1992), a local minimizer. Minimizations were checked using the Schwefel's evolution strategies method (Schwefel, 1995) which includes random probes in parameter space instead of settling on the first local minimum found. In no instance did we find that the random nonlocal minimizer found a value significantly smaller than that produced by the local minimizer. Moreover, the nonlocal minimizer tends to require about 20 times as many function evaluations.

3. Results

Results are described in four sections, each corresponding to a particular data set. Within each section, the smallest misfits attainable with the three models are compared.

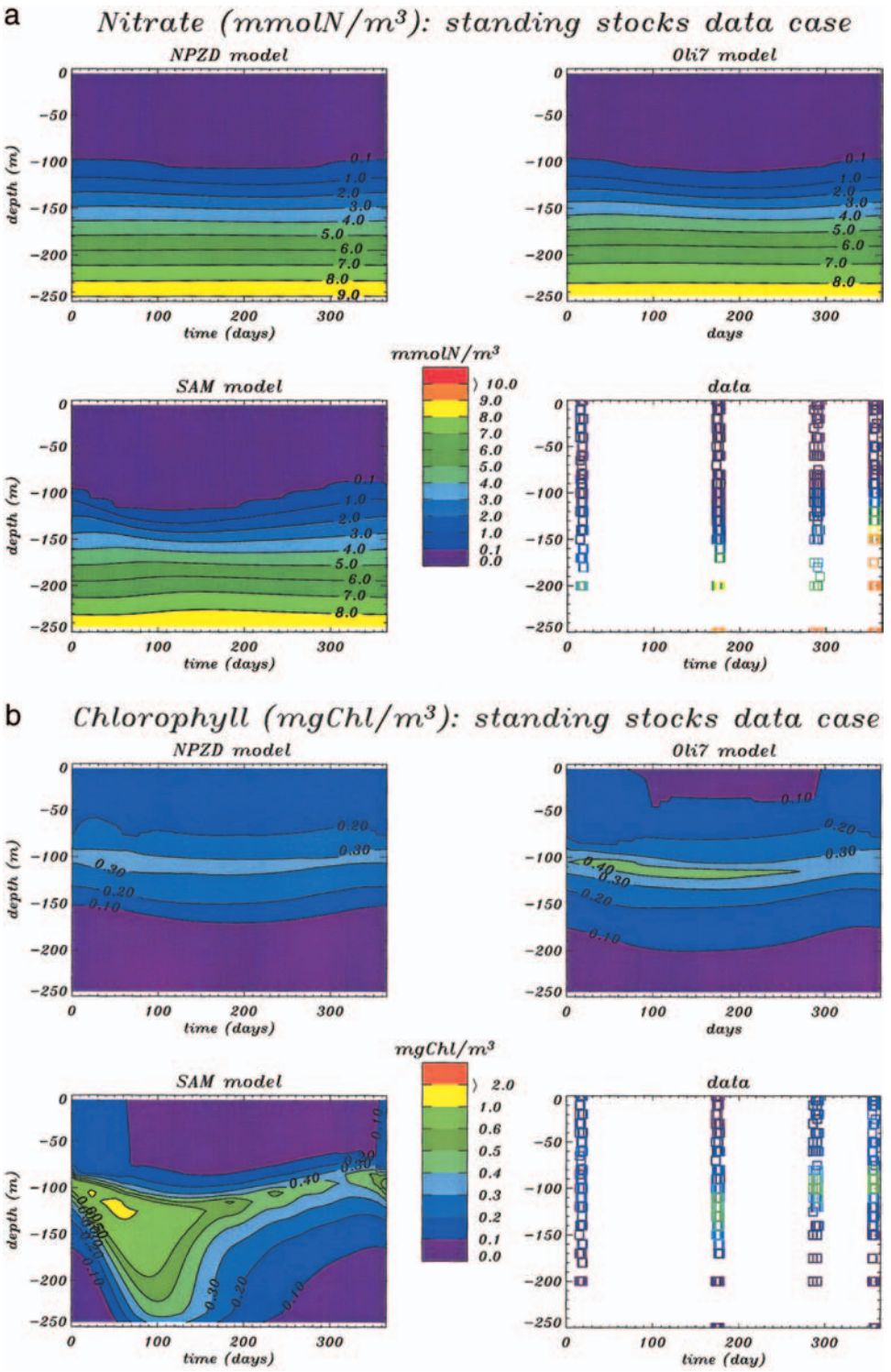

Figure 2. Evolution with time and depth for the three models and data of: (a) nitrate concentration (mmolN/m^3), (b) chlorophyll concentration (mgChl/m^3), (c) primary production (mmolN/m^3/d). Case for optimization with EUMELI standing stocks data (nitrate, chlorophyll and detritus data), the ncd case.

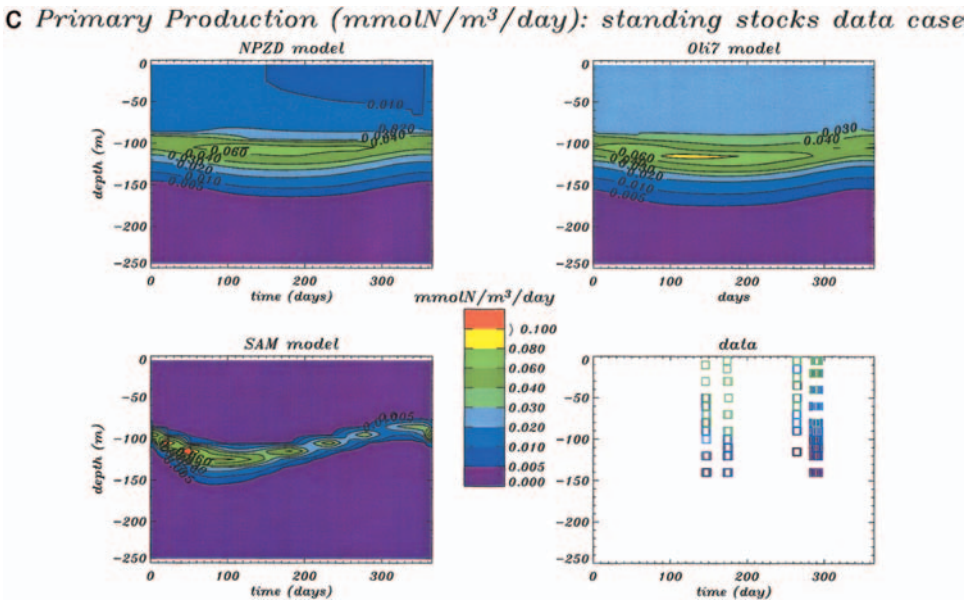

Figure 2. (Continued)

a. EUMELI standing stocks (ncd case)

In this case, the standing stock data (chlorophyll, nitrate and particulate nitrogen concentrations) are used for the optimization. Figure 2 shows the results obtained for each model. The model-data misfit is not very different for the three models: 25.6, 24.3, 25.9 for NPZD, Oli7 and SAM models, respectively.

Each model is able to reproduce the depleted nitrate ($<$0.1 mmolN/m^3) in the first 100 m (Fig. 2a). The nitracline is well reproduced by the three models. The seasonal depth variation of the nitracline is better captured by the SAM model. None of the three models is able to simulate the high nitrate concentration values at 250 m specially during EUMELI 5 (day 350–365), which could be expected, as the vertical 255 m level represents a boundary condition (fixed value with time).

Evolution of the chlorophyll concentration with time and depth (Fig. 2b) differs markedly for each model. For the NPZD model, the vertical distribution of chlorophyll remains quite stable over time. In the top 100 m, chlorophyll concentration ranges between 0.1–0.2 mgChl/m^3. In the observations, low values ($<$0.1 mgChl/m^3) are found during periods of water column stratification. The modelled concentrations in the deep chlorophyll maximum (DCM) are too low ($<$0.4 mgChl/m^3). For the Oli7 model, seasonality of chlorophyll concentration in the upper 100 m is well reproduced. The chlorophyll concentration in the DCM is slightly too low (0.4–0.5 mgChl/m^3). The position of the DCM is constant. The response of the SAM model presents a strong seasonality. Chlorophyll freshly produced in winter time is exported deeper down by sinking phytoplankton

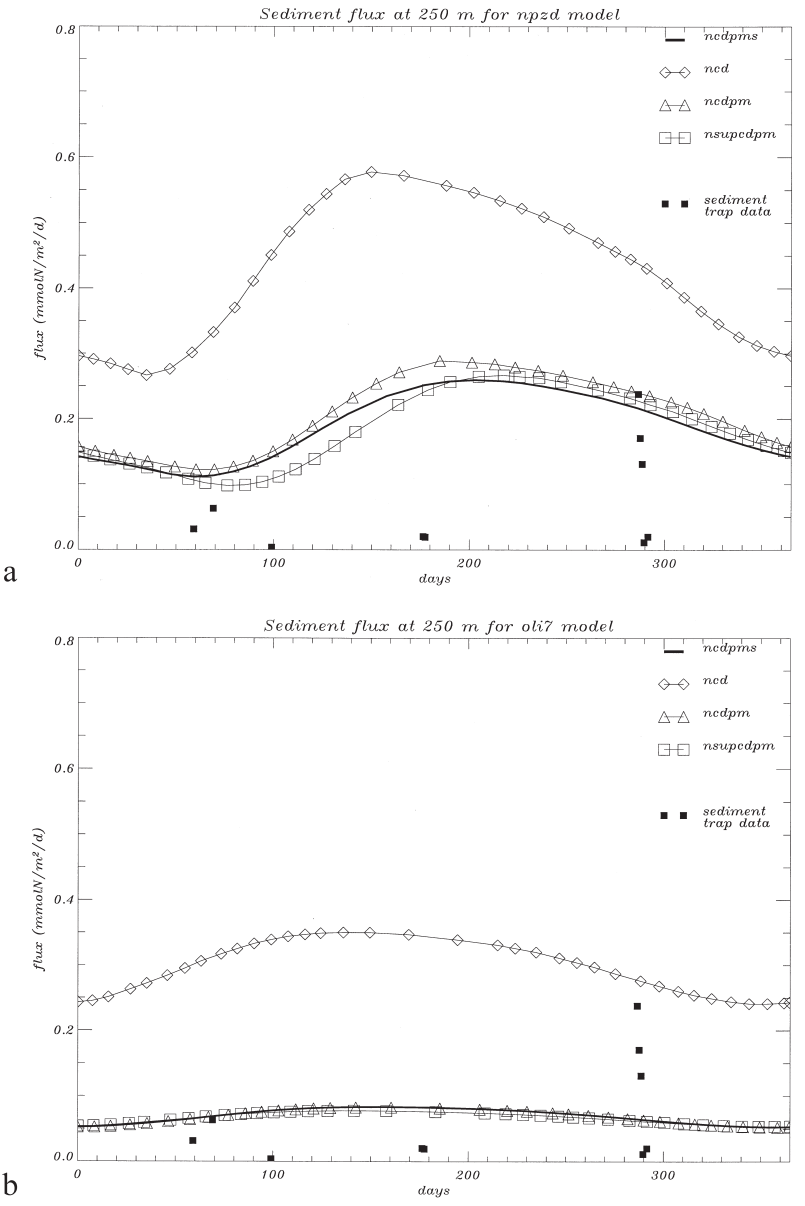

Figure 3. Evolution with time of sediment trap fluxes at 250 m depth for the different simulations (ncd, ncdpm, nsupcdpm, ncdpms) and models. Sediment trap data are plotted with black squares. (a) NPZD model, (b) Oli7 model and (c) SAM model. Ncd, ncdpm, nsupcdpm, ncdpms stand for standing stock data (nitrate, chlorophyll and particulate nitrogen concentrations), standing stocks plus rate data (primary production and sediment flux), the same data set than in previous case but without nitrate data below 130 m depth, and standing stocks plus rate plus SeaWiFS data, respectively.

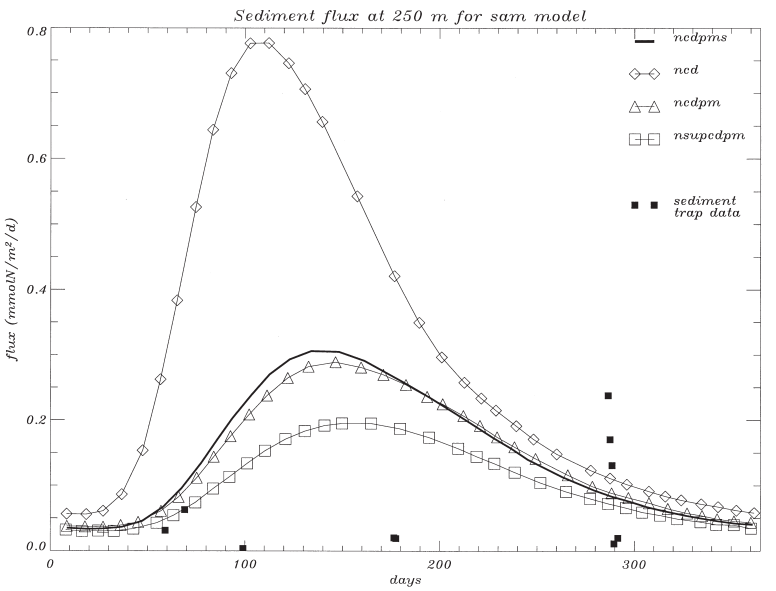

c

Figure 3. (Continued)

aggregates. The chlorophyll concentration in the DCM is too high (up to 1 mgChl/m^3) during winter and spring time. From the end of spring (May–June) until autumn, the DCM position varies from 120 m to 90 m, in agreement with the observed DCM position.

b. Prediction of measurements not used in the fitting for the ncd case

Other important quantities to analyze for biogeochemistry are the primary production and the sediment fluxes. Integrated annual primary production is equal to 98 (1173), 146 (1742), 34 (405) gC/m^2/yr (mmolN/m^2/yr) for NPZD, Oli7 and SAM models, respectively. Morel *et al.*'s (1996) estimation at the O-site from satellite data reaches a value of 110 gC/m^2/yr. Primary production is thus overestimated by the Oli7 model and underestimated by the SAM model. NPZD-modeled primary production is close to Morel *et al.*'s estimation. None of the three models is able to reproduce the decrease with depth of the primary production observations (Fig. 2c). All three models simulate a deep maximum of primary production associated with the DCM. Only the Oli7 model simulates primary production between 0.02 and 0.03 mmolN/m^3/d in the upper layer. The annual integrated sediment flux across the bottom of the modelled water column (250 m) is very high for the three models, above 100 mmolN/m^2/yr (110 for both Oli7 and SAM models and 158 mmolN/m^2/yr for NPZD model) which seems unrealistic at this site, observations indicating 43 mmolN/m^2/yr. Let us compare the model's results with the sediment trap data despite the scarcity of data. The sediment flux presents a high seasonality with a peak in summer for the NPZD model and spring for the SAM model (Fig. 3a, 3c). Oli7 model

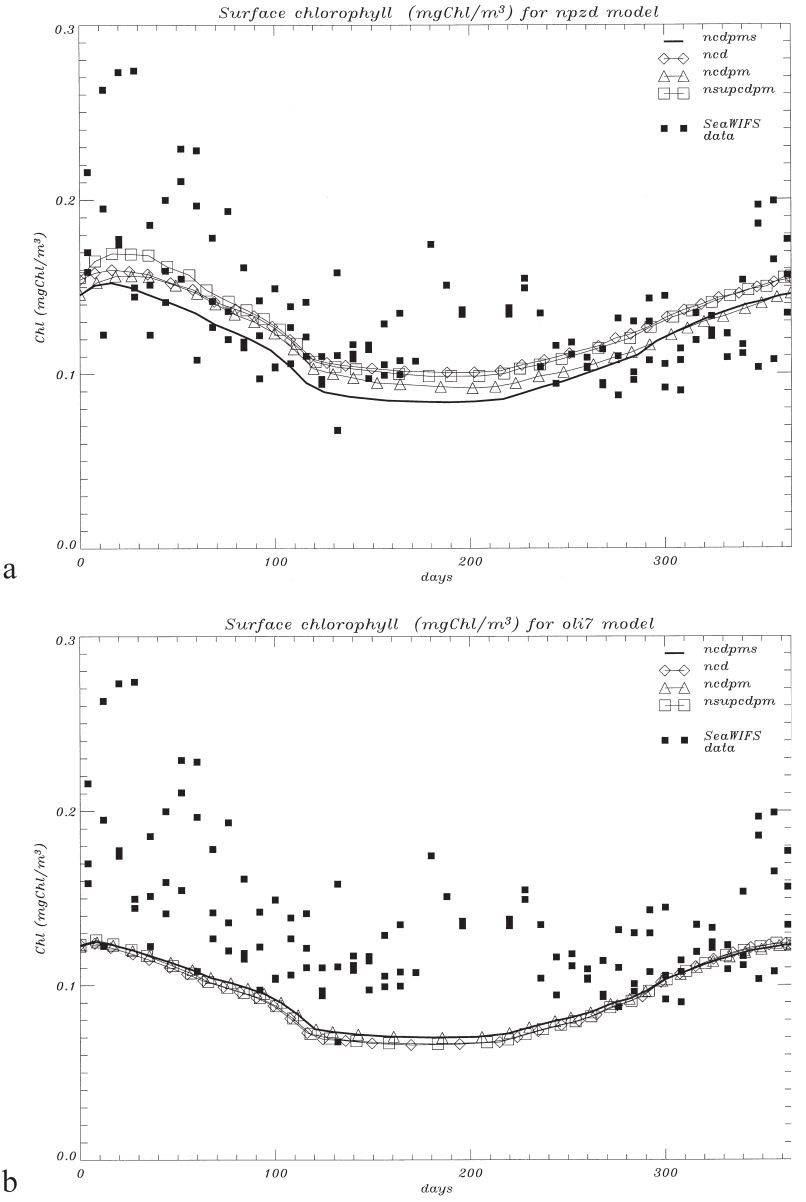

Figure 4. Evolution with time of chlorophyll concentration in the first 10 meters for the different simulations (see Fig. 3) for (a) NPZD model, (b) Oli7 model and (c) SAM model. SeaWiFS data are plotted with black squares.

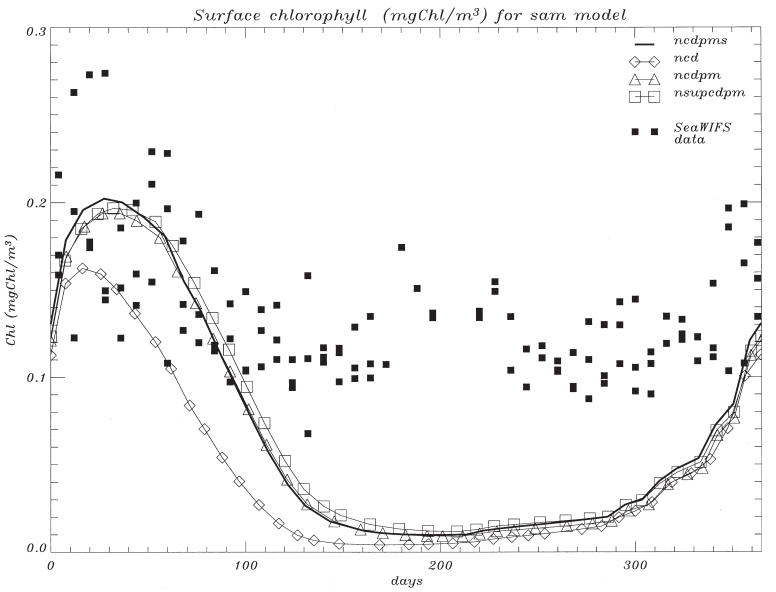

c

Figure 4. (Continued)

results (Fig. 3b) present a low variability.

For the SeaWiFS data, the high concentration in winter time is simulated only by the SAM model but this model is unable to reproduce the concentration level in summer time, the SAM chlorophyll level being low near 0.02 mgChl/m^3 (Fig. 4c). Good compromises are presented by the NPZD and Oli7 models with moderate increase during winter and concentrations near 0.1 mgChl/m^3 during summer time (Fig. 4a and 4b). The NPZD and SAM models results exhibit a marked seasonal character which we cannot detect in the observations.

c. Plus EUMELI rates (ncdpm case)

Particularly in an area of little seasonal variability, there is always the worry that a model will get the standing stocks approximately right while getting the flows among components completely wrong. Thus, even a few measurements of rates may provide good ability to distinguish among models. We included standing stocks and fluxes (primary production, sediment trap data at 250 m). We will explain the main differences for chlorophyll, nitrate and primary production (not shown) compared with the previous case. The model-data misfits for the three models are quite similar with values of 30, 27.2 and 31.3 for NPZD, Oli7 and SAM models, respectively.

The nitrate distribution is the same as in the previous case except at depth greater than 200 m. Near 200 m, nitrate concentrations are lower (5–6 mmolN/m^3) as the deep (250 m) nitrate reservoir parameter (N_{deep}) found by the optimization has decreased, as compared

Table 1. Parameters values for the optimization with all data (ncdpms case). The different columns represent the estimated, target (P^*) values, lower (P_0) and upper (P_1) bounds, weights (W), and Optimized (1) or not optimized (0) parameters. (a) for the NPZD model, (b) for the Oli7 model, (c) for the SAM model.

Estimated	P^*	P_0	P_1	W	Op	Notation	Definition	Unit
Table 1a								
0.053	0.1	0.001	1.	0.1	1	K_N	Half saturation concentration for nutrient uptake	mmolN/m^3
0.059	0.02	0.0	0.1	0.1	1	λ_{PN}	Phytoplankton exudation rate	d^{-1}
0.0038	0.02	0.0	0.1	0.1	1	λ_{PD}	Phytoplankton mortality rate	d^{-1}
3.4	2.0	1.0	5.0	0.1	1	μ_P	Maximum phytoplankton growth rate	d^{-1}
0.07	0.06	0.01	0.5	0.1	1	α	Initial slope of P-I curve	(W/m^2)$^{-1}$d^{-1}
0.95	1.	0.	2.	0.1	1	μ_Z	Maximum zooplankton grazing rate	d^{-1}
0.46	1.	0.1	3.	0.1	1	K_z	Half-saturation concentration for zooplankton grazing	mmolN/m^3
0.03	0.05	0.01	0.15	0.1	1	λ_{ZN}	Zooplankton excretion rate	d^{-1}
0.9	0.75	0.7	1.0	0.1	1	a	Assimilation efficiency of zooplankton	—
0.05	0.1	0.0	0.4	0.1	1	κ_{ZD}	(Quadratic) zooplankton mortality	(mmolN/m^3)$^{-1}$d^{-1}
0.018	0.02	0.0	0.2	0.1	1	λ_{DN}	Remineralization rate	d^{-1}
0.024	0.03	0.02	0.3	0.05	1	Kc	Light attenuation coefficient of chlorophyll	m^{-1}(mgChl/m^3)$^{-1}$
0.032	0.04	0.03	0.05	0.1	1	Kw	Light attenuation coefficient of pure water	m^{-1}
0.35	0.25	0.1	1	0.03	1	a_0	Minimum value of N:Chl ratio	molN/gChl
0.0081	.003	0.	0.01	0.03	1	a_1	Slope of N:Chl as a function of light (I)	(molN/gChl)/(W/m^2)$^{-1}$/d^{-1}

Table 1. (Continued)

Estimated	P^*	P_0	P_1	W	Op	Notation	Definition	Unit
7.44	9.8	6	17	0.1	1	N_{deep}	Deep nutrient pool	mmolN/m^3
2.63	1	0.	10.	0.05	1	V_D	Sinking velocity	m/d
0.67	0.6	0.4	0.8	0.1	1	f	Cloud fraction	—
Growth and grazing expressions:								
Phytoplankton growth rate: $J(z, t, N) = \mu_P \cdot min\left(J(z, t), \frac{N}{K_N + N}\right)$								
Growth rate without nutrient limitation: $J(z, t) = \frac{\alpha \cdot PAR}{\mu_P + \alpha \cdot PAR}$ with $PAR = 0.5 \cdot I(z)$ and $I(z) = I(0) \cdot \exp[-(Kw \cdot z + Kc \int_z^0 Chl(z, t)dz)]$								
Chlorophyll concentration estimation: $Chl(z, t) = \frac{N}{Chl}(z, day) \cdot P(z, t)$ with $N/Chl(z, day) = a_0 + a_1 \cdot \int_{day} I(z, t)dt$								
Zooplankton grazing expression: $G(P) = \frac{\mu_Z \cdot P^2}{K_Z^2 + P^2}$								
Table 1b								
0.054	0.1	0.001	1.	0.1	1	K_N	Half saturation concentration for nutrient uptake	mmolN/m^3
3.74	2.0	1.0	5.0	0.1	1	μ_P	Maximum phytoplankton growth rate	d^{-1}
0.13	0.06	0.01	0.5	0.1	1	α	Initial slope of P-I curve	(W/m^2)$^{-1}$d^{-1}
0.19	0.2	0.	0.4	0.1	1	γ	Fraction of primary production exuded	—
0.025	0.05	0.	0.1	0.1	1	λ_{PD1}	Phytoplankton mortality rate	d^{-1}
0.97	1.	0.	2.	0.1	1	μ_Z	Maximum zooplankton grazing rate	d^{-1}

Table 1. (Continued)

Estimated	P^*	P_0	P_1	W	Op	Notation	Definition	Unit
0.69	1.	0.1	3.	0.1	1	K_Z	Half-saturation concentration for zooplankton grazing	mmolN/m^3
0.97	0.9	0.	1.	0.1	1	$e1$	Preference of zooplankton for phytoplankton	—
0.03	0.1	0.	1.	0.1	1	$e2$	Preference of zooplankton for detritus	—
0.88	0.75	0.7	1.	0.1	1	a	Assimilation efficiency of zooplankton	—
0.95	0.75	0.0	1.0	0.05	1	α_a	Fraction of small particles as compared with large particles in fecal pellets	—
0.026	0.05	0.01	0.15	0.1	1	λ_{ZN}	Zooplankton excretion rate	d^{-1}
0.19	0.1	0.0	0.4	0.1	1	κ_{ZD}	(Quadratic) zooplankton mortality	(mmolN/m^3)/d
0.97	0.75	0.0	1.	0.05	1	α_D	Fraction of small particles as compared with large particles in zooplankton mortality	—
0.26	2.8	0.	15	0.05	1	$\mu 1$	Maximum hydrolysis rate of particles (D1 and D2) in labile DON	d^{-1}
8.63	1.5	0.	15	0.05	1	$Kr1$	Half-saturation constant associated with hydrolysis in labile DON	(mmolN/m^3)
5.44	0.28	0.	15	0.05	1	$\mu 2$	Maximum hydrolysis rate of particles (D1 and D2) in semi-labile DON	(mmolN/m^3)/d

Table 1. (Continued)

Estimated	P^*	P_0	P_1	W	Op	Notation	Definition	Unit
9.75	1.5	0.	15	0.05	1	$Kr2$	Half-saturation constant associated with hydrolysis in semi-labile DON	(mmolN/m^3)
0.215	0.215	0.215	0.215	1.	0	Bac	Bacterial biomass concentration	(mmolN/m^3)
0.30	0.5	0.1	4.	0.1	1	λ_{DON1N}	Remineralization rate of labile DON in nutrients	d^{-1}
0.0039	0.01	0.0027	0.1	0.1	1	λ_{DON2N}	Remineralization rate of semi-labile DON in nutrients	d^{-1}
0.022	0.03	0.02	.3	0.05	1	Kc	Light attenuation coefficient of chlorophyll	m^{-1}(mgChl/m^3)$^{-1}$
0.032	0.04	0.03	0.05	0.1	1	Kw	Light attenuation coefficient of pure water	m^{-1}
0.24	.25	0.1	1	.03	1	a_0	Minimum value of N:Chl ratio	molN/gChl
0.0054	.003	0.0	.01	.03	1	a_1	Slope of N:Chl as a function of light (I)	(molN/gChl)/(W/m^2)$^{-1}$/d
8.15	9.8	6.0	17.	0.1	1	N_{deep}	Deep nutrient pool	mmolN/m^3
3.074	1.	0.	10.	0.05	1	v	Sinking velocity of small particles	m/d
100	100.	10.	300.	0.05	0	V	Sinking velocity of large particles	m/d
0.55	0.6	0.4	0.8	0.1	1	f	Cloud fraction	—
Growth and grazing expressions:								
Phytoplankton growth rate: $J(z, t, N) = \mu_P \cdot J(z, t) \cdot \dfrac{N}{K_N + N}$								

Table 1. (Continued)

Estimated	P^*	P_0	P_1	W	Op	Notation	Definition	Unit
Growth rate without nutrient limitation: $J(z,t) = \frac{\alpha \cdot PAR}{\mu_P + \alpha \cdot PAR}$ with $PAR = 0.5 \cdot I(z)$ and $I(z) = I(0) \cdot \exp[-(Kw \cdot z + Kc \int_z^0 Chl(z,t)dz)]$								
Chlorophyll concentration estimation: $Chl(z,t) = \frac{N}{Chl}(z, day) \cdot P(z,t)$ with $N/Chl(z, day) = a_0 + a_1 \cdot \int_{day} I(z,t)dt$								
Zooplankton grazing expression G: $G(P) + G(D) = \left(\frac{e1 \cdot P^2}{K_Z \cdot (e1 \cdot P + e2 \cdot D1) + e1 \cdot P^2 + e2 \cdot D1^2} + \frac{e2 \cdot D1^2}{K_Z \cdot (e1 \cdot P + e2 \cdot D1) + e1 \cdot P^2 + e2 \cdot D1^2} \right)$								
Table 1c								
0.079	0.1	0.001	1	0.1	1	K_N	Half saturation concentration for nutrient uptake	mmolN/m^3
1.84	2	1	5	0.1	1	μ_P	Maximum phytoplankton growth rate	d^{-1}
0.37	0.06	0.01	0.5	0.1	1	α	Initial slope of P-I curve	(W/m^2)$^{-1}$d^{-1}
0.018	0.02	0	0.1	0.1	1	λ_{PN}	Phytoplankton exudation rate	d^{-1}
0.008	0.015	0.005	0.3	0.05	1	Kc	Light attenuation coefficient of chlorophyll	m^{-1}(mgChl/m^3)$^{-1}$
0.017	0.015	0.005	0.3	0.05	1	Kd	Light attenuation coefficient of aggregates	m^{-1}(m^{-3})$^{-1}$
0.033	0.04	0.03	0.05	0.1	1	Kw	Light attenuation coefficient of water	m^{-1}
0.93	0.25	0.1	1	0.03	1	a_0	Minimum value of N:Chl ratio	molN/gChl
0.001	0.003	0.	.01	0.03	1	a_1	Slope of N:Chl as a function of light (I)	(molN/gChl)/(W/m^2)/d
7.45	9.8	6	17	0.1	1	N_{deep}	Deep nutrient pool	mmolN/m^3

Table 1. (Continued)

Estimated	P^*	P_0	P_1	W	Op	Notation	Definition	Unit
0.002	0.002	0.001	0.003	0.1	0	m	Cell diameter	cm
0.009	0.004	0.001	0.02	0.1	1	C_m	Cell mass	nM
1.92	2.28	1.5	3	0.1	1	n	Fractal dimension	—
0.116	0.6	0.03	3	0.1	1	v	Cell sinking velocity	m/d
0.392	1.17	0.16	2.18	0.1	1	η	Sinking exponent	—
2	2	1	3	0.1	0	M	Upper bound for aggregate diameter	cm
0.97	0.9	0.09	1	0.1	1	b	Separation probability	—
1.4	0.84	0.2	2	0.1	1	$shear$	Shear rate	s^{-1}
0.49	0.05	0.01	0.7	0.1	1	$stick$	Stickiness	—
0.55	0.6	0.4	0.8	0.1	1	f	Cloudiness	—
Photosynthesis:								
Phytoplankton growth rate: $J(z, t, N) = \mu_P \cdot min\left(J(z, t), \frac{N}{K_N + N}\right)$								
Growth rate without nutrient limitation: $J(z, t) = \frac{\alpha \cdot PAR}{\mu_P + \alpha \cdot PAR}$ with $PAR = 0.5 \cdot I(z)$ and $I(z) = I(0) \cdot exp[-(Kw \cdot z + Kc \int_z^0 Chl(z, t)dz + Kd \int_z^0 PHYNOS(z, t)dz)]$								
Chlorophyll concentration estimation: $Chl(z, t) = \frac{N}{Chl}(z, day) \cdot P(z, t)$ with $N/Chl(z, day) = a_0 + a_1 \cdot \int_{day} I(z, t)dt$								

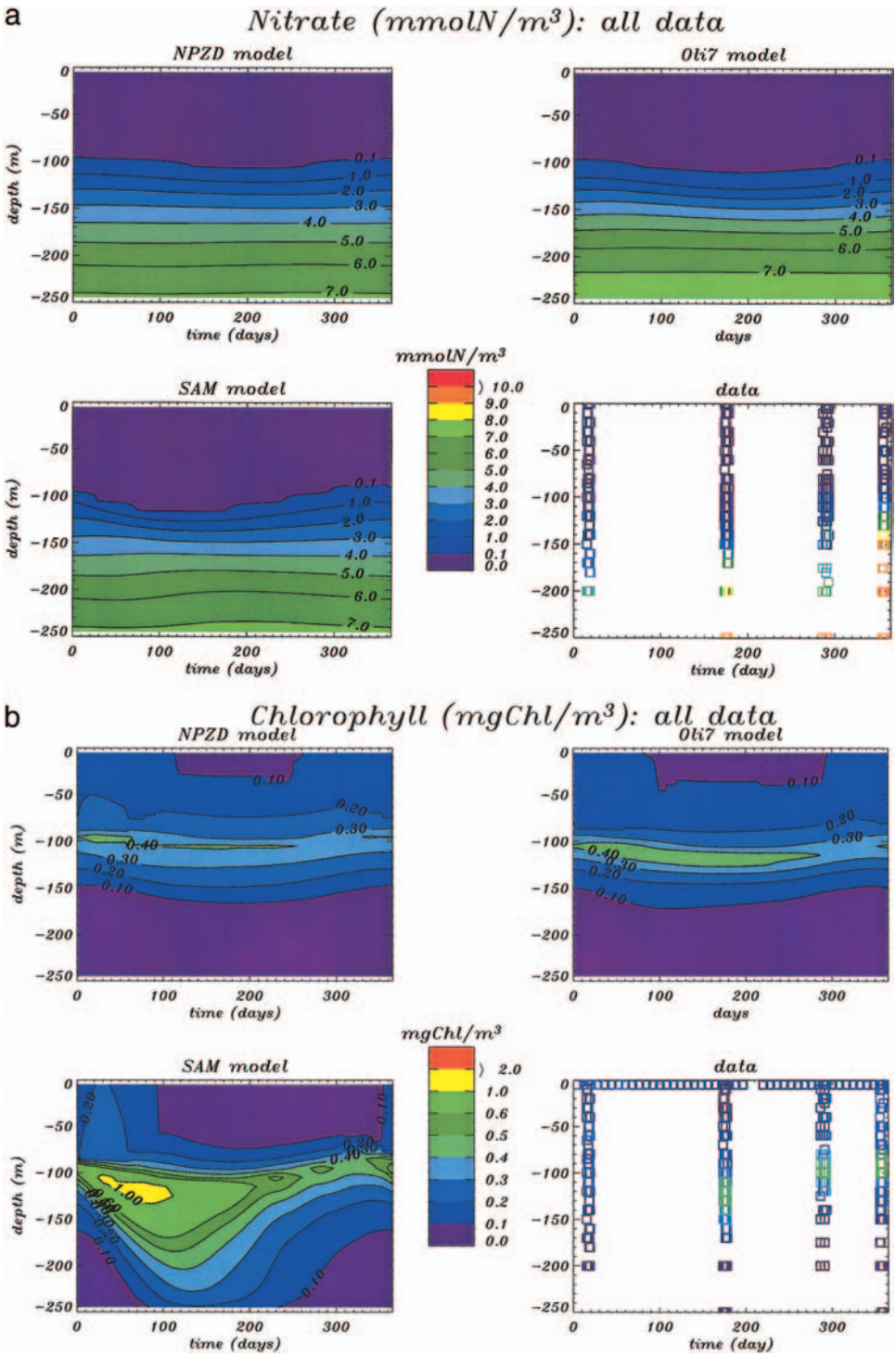

Figure 5. Same as Figure 2. Case for optimization with EUMELI standing stocks (nitrate, chlorophyll and particulate nitrogen), rates (primary production and sediment flux) and SeaWiFS data.

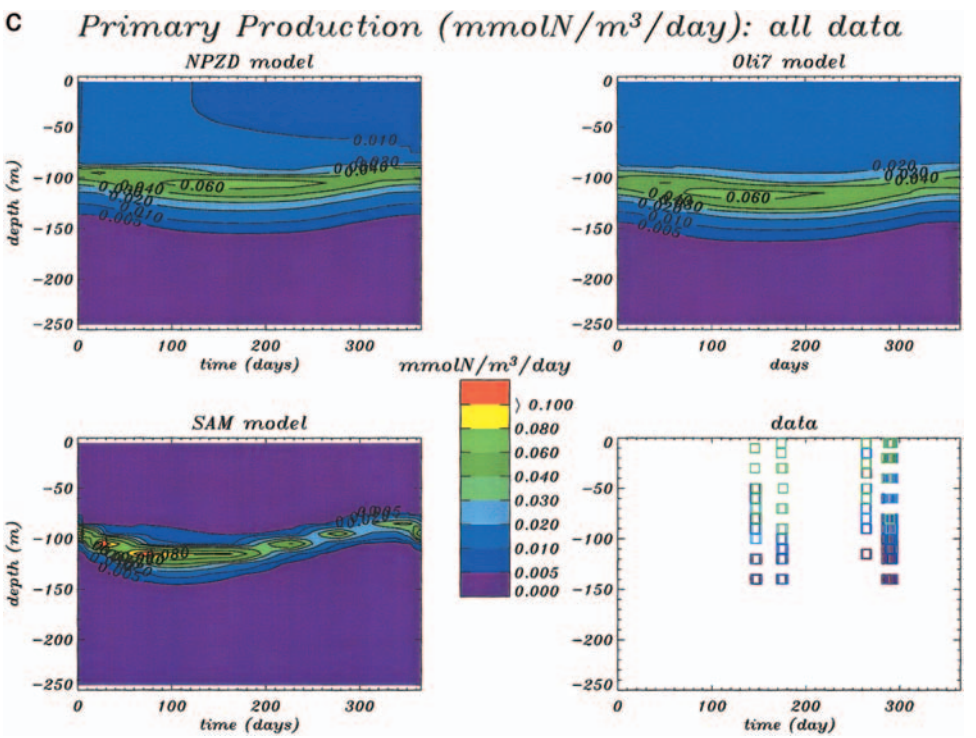

Figure 5. (Continued)

with the previous case, from 9–9.5 to 7.5–8 mmolN/m^3. For both Oli7 and NPZD models, the chlorophyll gradient under the DCM is stronger. The DCM concentration in the water column for the SAM model is not as high as in the previous case. The annual integrated primary production varies slightly with values of: 84 (1003), 97 (1152) and 39 (466) gC/m^2/yr (mmolN/m^2/yr) for NPZD, Oli7 and SAM models, respectively. Despite the introduction of primary production observations in the data set used for the optimization, the position of the DCM is still associated with the modeled maximum of primary production. The annual sediment flux at 250 m is decreased now to values of 76, 25.5, 52 mmolN/m^2/yr for NPZD, Oli7 and Sam, respectively. The NPZD integrated flux is still too high as compared with observations (43 mmolN/m^2/yr). The excessive seasonal cycle for the NPZD and SAM model sediment trap flux is much reduced (Fig. 3a, 3c). Introduction of sediment trap data in the optimization data set seems to be important at this site. However, we have to remember that large uncertainties remain about shallow sediment trap data for the estimation of particle flux (Baker *et al.,* 1988; Knauer and Asper, 1989; Bacon, 1996). Surface chlorophyll variability does not differ from the previous case for Oli7 and NPZD models (Fig. 4a and 4b). SAM model chlorophyll concentration is higher in winter time (closer to data) (Fig. 4c).

d. Plus SeaWiFS standing stocks (ncdpms case)

The data set used for optimization includes now nitrate, chlorophyll, particulate nitrogen, primary production, sediment trap fluxes and also SeaWiFS data. Tables 1a, 1b, 1c provide the optimized parameters sets found for the three models with this data set (all data presented in Section 2a).

The vertical distribution of chlorophyll, nitrate and primary production (Fig. 5a,b,c) are very similar to the ncdpm case. For surface chlorophyll, the regular SeaWiFS surface chlorophyll distribution yields an increase in the chlorophyll concentration for Oli7 model and specially SAM model during the winter season (Fig. 4b and 4c). With all available data used for the optimization, Oli7 model primary production is closer to observations with 97 (1152) gC/m^2/yr (mmolN/m^2/yr), (82 (974) and 40 (474) gC/m^2/yr (mmolN/m^2/yr) for NPZD and SAM models, respectively). The annual sediment flux decreases for NPZD and Oli7 models (69.1 and 25.4 mmolN/m^2/yr, respectively) and slightly increases for the SAM model (53.4 mmolN/m^2/yr). The sediment flux time evolution at 250 m is similar than in the ncdpm case (Fig. 3a,b,c).

The model-data misfit values are again quite comparable for the three models: 30.1, 27.3, 31.7 for NPZD, Oli7 and SAM models, respectively.

e. Partitioning of misfit for the ncdpms case

The different type of data do not contribute the same manner to the total misfit between observations and model predictions given the chosen misfit function (Table 2). 62 to 80% of the total misfit for the whole column is due to nitrate concentrations depending on the models; the major contribution being the nitrate contribution below 130 m, followed by the mid-depth nitrate concentrations. Contributions (higher than 5%) of the other data types in the total misfit differ depending on the model (Table 2). For NPZD model, deep particulate nitrogen and sediment flux constitute the main factors. Oli7 model misfit originates in deep particulate nitrogen and shallow nitrate. For SAM model, shallow particulate nitrogen, sediment flux and shallow primary production constitute the main players.

f. Influence of deep nitrate concentration (below 130 m) (nsupcdpm case)

Deep nitrate concentrations are the main contributor to the misfit value for the three models. We noticed in Section 2b that deep nitrate concentrations below 130 m vary significantly seasonally. What is the influence of deep nitrate values below 130 m on the results? We address this question through a sensitivity test: We withdrew the nitrate concentrations below 130 m from the data set used for the optimization (standing stocks and rates, the ncdpm case). The only resulting difference is a decrease of modeled deep nitrate concentrations. Deep nitrate concentrations do not appear to control the behaviour of the models in terms of chlorophyll, nitrate above 130 m and primary production distributions. The main impact is on the annual integrated sediment flux which is reduced by 11%, 4% and 28% for NPZD, Oli7 and SAM models, respectively relative to ncdpm. The influence of withdrawing deep NO_3 data from the optimization data set is clearly seen

Table 2. Contribution of different types of observations to the total misfit for the three models for the optimization with all data. *N*, *Chl*, *PN*, *PP*, Deep mooring stand for nutrient concentration, chlorophyll concentration, particulate nitrogen concentration, primary production and sediment trap fluxes, respectively. Points indicate the number of observations used in each case. In the 3rd, 4th and 5th columns, the contribution of each type of observation to the total misfit for the three models is expressed in nondimensional units. The percentage with respect to the total misfit is given in the parentheses.

Data set total	Points 1413	NPZD misfit 30.1	Oli7 misfit 27.3	Sam misfit 31.7
NO_3 shallow $\leq$ 100 m	226	1.45 (4.8%)	1.7 (6.2%)	0.9 (2.8%)
mid depth 100–130 m	85	8.5 (28.2%)	7.5 (27.5%)	5.5 (17.5%)
deep $>$ 130 m	125	13.82 (46%)	12.7 (46.5%)	13.4 (42.3%)
Chl shallow $\leq$ 100 m	220	0.22 (0.73%)	0.25 (0.92%)	0.54 (1.7%)
deep $>$ 100 m	198	0.2 (0.66%)	0.25 (0.92%)	1.3 (4.1%)
ocean color	120	0.0035 (0.01%)	0.07 (0.26%)	0.31 (0.95%)
PN shallow $\leq$ 100 m	156	1.3 (4.5%)	0.92 (3.4%)	4.8 (15.1%)
deep $>$ 100 m	149	1.85 (6.1%)	2.0 (7.3%)	1.1 (3.5%)
PP shallow $\leq$ 100 m	92	0.55 (1.8%)	0.33 (1.2%)	1.6 (5%)
deep $>$ 100 m	32	0.6 (2%)	0.74 (2.7%)	0.15 (0.45%)
Deep mooring (250 m)	10	1.56 (5.2%)	0.84 (3.1%)	2.1 (6.6%)

on the modeled sediment flux at 250 m. An increase of primary production appears for NPZD and Oli7 models (12%, 2%) and a small decrease for the SAM model (1%).

4. Discussion

The original hope, that lateral effects were small enough that a one-dimensional observational and modeling study would suffice, was not met. This is discouraging, because it implies that a vastly greater effort, both in ships and in computation, will be needed to provide a useful reduction in uncertainty about the processes and rate parameters of biogeochemistry. However, we decided to keep this simple one-dimensional physical frame to test and analyze the performance of the three models in a first step. It will be very interesting to confirm or to show up the weakness of these results in a three-dimensional frame which will be, however, much more costly in computer time, especially with the global optimization method used in the present paper.

Evans (2003) demonstrated that defining misfit can have a large influence on the "best" estimate of biogeochemically important fluxes and concentrations. We decided in this paper to use a weighting scheme based on the overall range for a given data type as we were interested more in major biogeochemical features than in ecological details.

The models had different numbers of estimated parameters (18 for NPZD, 29 for Oli7,

Table 3. Common parameters values for the three models for the optimization with all data (ncdpms case). The different columns represent name of parameters, definitions, estimated values for NPZD (P_{NPZD}), Oli7 (P_{Oli7}), SAM (P_{Sam}), and $f1 = max\ (P_{Sam}, P_{NPZD}, P_{Oli7})$/min ($P_{Sam}$, P_{NPZD}, P_{Oli7}), $f2 = P_1/P_0$.

Parameters	Definitions	P_{NPZD}	P_{Oli7}	P_{Sam}	$f1$	$f2$
K_N	Half-saturation for nitrate uptake	0.053	0.054	0.079	1.5	1000
μ_P	Maximum growth rate of phytoplankton	3.40	3.74	1.84	2	5.
α	Initial slope of P-I curve	0.07	0.13	0.37	5	50.
λ_{PN}	Phytoplankton exudation rate	0.059	—	0.018	3	∞
Kc	Light attenuation coefficient of chlorophyll	0.024	0.022	0.017	1.4	15
Kw	Light attenuation coefficient of water	0.032	0.032	0.033	1	1.6
a_0	$N/Chl = a_0 +$	0.35	0.24	0.93	4	10
a_1	$+ a_1 \times Imoy(z, t)$	0.0081	0.0054	0.001	8	∞
N_{deep}	Deep NO_3 concentration under 250 m	7.44	8.15	7.45	1.1	2.83
f	Fractional cloud cover	0.67	0.55	0.55	1.2	2.

20 for SAM), which might be used with an information criterion to guide model selection, if we were much more sure than we are about the statistical distribution of observational errors and model misspecifications.

a. Common parameters values between the three models

For the full data set, do common parameters of the three models obtain the same values after optimization? Can we propose consistent parameter values for some biogeochemical processes?

In the three models, photosynthesis is represented by the same formulation (Evans and Parslow, 1985) and nutrient limitation by the same Michaelis-Menten formulation. However, in the Oli7 model, the product of nutrient and light limitation terms is considered and the NPZD and SAM models use the lesser of the two limiting factors. Maximum phytoplankton growth rate (μ_P) and half-saturation constant for nutrient uptake (K_N) are quite comparable for NPZD and Oli7 models, 3.4–3.7 day^{-1} and 0.053–0.054 $mmolN/m^3$, respectively (Table 3). Indeed, the largest range of values found by the three models ($f1$) ends up usually much smaller than the original range ($f2$) (see Table 3), especially for K_N. For the SAM model, the solution found is different, maybe due to the very different trophic structure of this model. The initial slope of the P-I curve is very different for the three models within a factor of five between the smallest and largest values. Babin *et al.* (1996) and Morel *et al.* (1996) have measured physiological parameters derivable from photosynthesis-irradiance (P-I) curves, such as the maximum yield for growth, the irradiance level that determines the onset of the light saturated photosynthesis regime, the maximum rate of

production in this regime and the photosynthesis available irradiance (PAR) incident at sea level or within the water body. These data might be additional information for constraining the α initial slope of the P-I curve and the maximum phytoplankton growth rate. It will be interesting to investigate the impact of these data in a future study.

The other common parameters with quite comparable values are the water attenuation coefficient (Kw) with 0.032–0.033 m^{-1} and the chlorophyll attenuation (Kc) with 0.022–0.024 $m^{-1}(mgChl/m^3)^{-1}$. For the SAM model, the chlorophyll attenuation is smaller because the aggregate attenuation is also taken into account. Deep nitrate pool (N_{deep}) and cloud fraction (f) have also similar values. The largest differences are found for parameters linked to the N/Chl ratio parameterization (Table 3), specially for the slope of this ratio (a_1) as a function of available light for cells. It could be mainly attributed to missing phytoplankton nitrogen data for constraining this ratio.

b. Effect of different data type on parameter estimations

When primary production (PP) and sediment fluxes data are included in the data set used for the optimization (ncdpm case), the modeled particulate flux at 250 m decreases for the three models (Fig. 6). For the modeled PP, a small decrease is noticed for NPZD and Oli7 models, and a small increase for SAM model (Fig. 6). Models can be tuned to yield the observed vertically integrated primary production but not the observed high values near the surface. It must be remembered that primary production computed in the model is what contributes to growth and reproduction of cells, whereas primary production as measured can include carbon that is fixed and then, in the absence of fixed nitrogen to combine with for growth, exuded as organic carbon without contributing to reproduction. Given the apparent lack of nitrogen for cell growth in surface water where observed primary production is higher than that modeled, it seems plausible that "nongrowth" primary production constitutes much of what is measured near the surface.

For the NPZD model, the decrease by a factor of two of the particulate flux at 250 m is linked to a decrease of the detritus sinking speed value (V_D) and to a large increase of the detritus remineralization rate (λ_{DN}) (Fig. 6). The small PP decrease is linked mainly to a moderate decrease of the initial slope of P-I curve (not shown). For the Oli7 model, the decrease of PP results from a reduced fueling in nitrates from several routes: a reduced zooplankton excretion (λ_{ZN}) and a reduced semi-labile DOM pool due to an increase in the hydrolysis ($Kr1$, $Kr2$) of small and large particles. The increased fraction of exuded PP (γ) is counterbalanced by the decreased remineralization (λ_{DON1N}, λ_{DON2N}, not shown) of both *DON1* and *DON2*. The decrease in both the zooplankton production of fecal pellets ($1 - a$) and the maximum zooplankton grazing (μ_Z, not shown) yields a reduced particulate flux at 250 m (Fig. 6). For the SAM model, the maximum phytoplankton growth rate (μ_P) decrease should induce a PP decrease. However, PP increases slightly, certainly linked to a less severe nutrient limitation, the half-saturation concentration for nutrient uptake (K_N) having decreased. The decrease in the cell sinking velocity induces a reduced particulate flux at 250 m (Fig. 6).

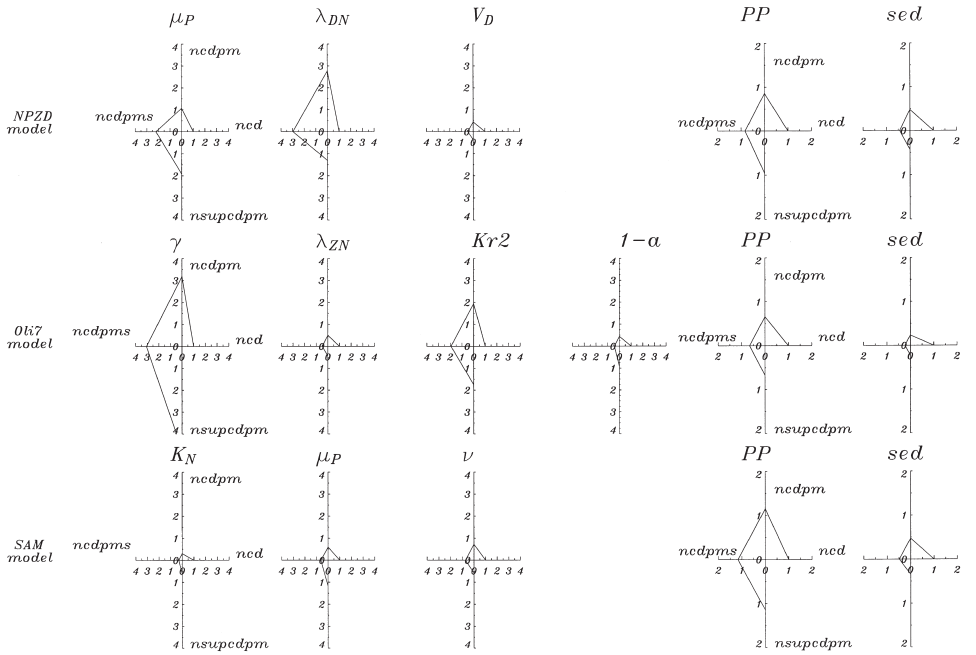

Figure 6. Comparisons of model parameters, primary production (PP) and sediment fluxes (sed) values for the ncd (east axis), ncdpm (north axis), ncdpms (west axis) and nsupcdpm (south axis) cases. Each variable value has been normalized by the ncd case value for the same variable. Only parameters whose values change within a factor two or more between the four cases have been considered here. Upper, middle and lower panels of the figure correspond to the NPZD, Oli7 and SAM models, respectively.

Inclusion of SeaWiFS data within the *in situ* data set (which already includes surface chlorophyll measurements) does not induce important change in parameters values for the three models. We have shown that sediment flux and primary production data contain very useful information despite their scarcity. For the three models, the modeled sediment flux at 250 m has been divided by a factor two to four in better agreement with the data. Introduction of the primary production data in the optimization procedure constrains the models to maintain a moderate primary production level.

c. Importance of the DON pool

The Oli7 model is the only model which takes explicitly into account dissolved organic nitrogen with two fractions: labile (turnover rate: $\tau \sim$ hours–days) and semi-labile ($\tau \sim$ months) (Carlson and Ducklow, 1995). DON data (not used in the optimization procedure) can be compared with the modeled DON concentrations. The nitrogen content of the labile DOM was estimated by considering it equal to the total dissolved amino-acid concentrations (Dadou *et al.,* 2001). The simulated labile DON is underestimated (lower than

0.1 mmolN/m^3) compared with data (0.1 to 0.3 mmolN/m^3 (Martin-Jézéquel, pers. com.). The semi-labile pool is estimated by subtracting the refractory DOM concentration ($\tau \sim$ 4000–6000 yr; Bauer *et al.,* 1992), which is assumed to exhibit a constant concentration (3 mmolN/m^3) with depth, from the DOM measurements (Dadou *et al.,* 2001). Modeled semi-labile DON presents concentrations comparable with data between 1.5 and 3 mmolN/m^3 in the first 100 meters and a maximum localized at the same depth than the DCM with a value around 0.3 mmolN/m^3. The turnover rate of labile DON for different optimization data sets is quite robust: between 2.4 days (ncd case) and 3.3 days (ncdpms case). The semi-labile DON turnover rate is more variable with the different optimization data sets ranging between 4.7 and 8.2 months. It equals 4.7 months for the ncd case experiment yielding a higher primary production than in the ncdpm data experiment where the turnover rate equals 8.2 months.

The other models (NPZD and Sam) are not able to reproduce an annual primary production close to 110 gC/m^2/yr when all data are used in the optimization procedure. Our NPZD model presents a return flux from the phytoplankton pool to the nutrient pool mimicking a DON pool without residence time, instantaneously converted in nutrients. This NPZD version, modified from Oschlies *et al.* (2000), optimized for the EUMELI oligotrophic site, is able to simulate a substantial primary production compared to the Oschlies *et al.* (2000) version embedded in an eddy-permitting three dimensional model of the entire North Atlantic ocean. Our results confirm that the DOM plays a major role in this subtropical region of the North Atlantic ocean. The semi-labile DOM in the upper layer remineralizes slowly and constitutes a constant source of nutrients throughout the year.

d. The role of zooplankton

NPZD and Oli7 models have a zooplankton compartment, and we can compare the simulated zooplankton concentrations with data. However, no microzooplankton biomass was measured at the EUMELI O-site and the direct comparison of mesozooplankton measurements made during the EUMELI cruises with the zooplankton variable of the models is problematic since small size classes tend to dominate the food web at the O-site. During the Plankton 89 expedition, Passow and Peinert (1993) measured at 18N, 29W in early April 1989 integrated values of microzooplankton in the upper 80 m of 450 mgC/m^2 (0.056 mmolN/m^3). In the upper 80 m, the Oli7 and NPZD models estimate zooplankton concentrations between 0.2 and 0.15 mmolN/m^3, much higher than observations. It is wise to state that validation with zooplankton data is delicate at the O-site.

5. Conclusion

This study represents an attempt to use data assimilation and observations to estimate model parameters and compare three models of different complexity in a one-dimensional physical frame. By assimilating the EUMELI oligotrophic data (standing stocks, rates and SeaWiFS data), we were not able to decide among the different candidates based on their

misfit values. As Evans (2003) demonstrated, defining misfit can have a large influence on the "best" estimate of biogeochemically important fluxes and concentrations. When all data are used for the optimization, the three model misfits are quite comparable. Looking at the annual primary production (PP) and sediment flux, the Oli7 model is the only one which could maintain an annual PP around 100 $gC/m^2/yr$ (1155 $mmolN/m^2/yr$) and a moderate sediment flux around 26 $mmolN/m^2/yr$ comparable with the scarce available data. Some other biogeochemical features were well reproduced by the two other candidates. The SAM model is the only one able to simulate a seasonal deepening of the DCM. The NPZD model is able to model a substantial primary production without any explicit DOM pool representation.

In order to combine different positive features of each model, a new version of the Oli7 model could include only one semi-labile DON pool instead of two explicit pools in the present version, and a return flow from the phytoplankton pool to the nutrient pool mimicking the more labile DON. This new model could also incorporate new processes linked to the particles dynamics: aggregation-disaggregation of phytoplankton cells, of zooplankton fecal pellets and cadavers. This new model should be embedded into a three-dimensional physical model which resolves the eddy dynamics to study the influence of lateral advection on parameter estimates.

Acknowledgments. We especially want to thank all the scientists who performed the measurements during the EUMELI JGOFS-France program and made those measurements available to the community on the French JGOFS data base: http://www.obs-vlfr.fr/jgofs. We thank also the SeaWiFS team for chlorophyll data, Joël Sudre (LEGOS) for the SeaWiFS data extraction near the EUMELI O-site, as well as the two anonymous reviewers for their useful comments which improved the manuscript. This work was funded by the national PROOF modeling program. This work was initiated when Geoff Evans was a visiting scientist at LEGOS; financial support from the University Paul Sabatier is acknowledged.

REFERENCES

André, J. M. 1991. Télédétection spatiale de la couleur de la mer: Algorithmique d'inversion du Coastal Zone Color Scanner: Application à l'étude de la Méditerranée occidentale, PhD thesis, University Pierre and Marie Curie, 246 pp.

Babin, M., A. Morel, H. Claustre, A. Bricaud, Z. Kolber and P. Falkowski. 1996. Nitrogen- and irradiance-dependent variations of the maximum quantum yield of carbon fixation in eutrophic, mesotrophic and oligotrophic marine systems. Deep-Sea Res. I, *43,* 1241–1272.

Bacon, M. P. 1996. Evaluation of sediment traps with naturally occurring radionuclides, *in* Particle Flux in the Oceans, *57* SCOPE Report, V. Ittekkot, P. Schäfer, S. Honjo, and P. J. Depetris, eds., Wiley, NY, 85–90.

Baker, E. T., H. B. Milburn and D. A. Tennant. 1988. Field assessment of sediment trap efficiency under varying flow conditions. J. Mar. Res., *46,* 573–592.

Bauer, J. E., P. M. Williams and E. R. Druffel. 1992. ^{14}C activity of dissolved organic carbon fractions in the north-central Pacific and Sargasso Sea. Nature, *357,* 667–669.

Bory, A., C. Jeandel, N. Leblond, A. Vangriesheim, A. Khripounoff, L. Beaufort, C. Rabouille, E. Nicolas, K. Tachikawa, H. Etcheber and P. Buat-Ménard. 2001. Downward particle fluxes within different productivity regimes off the Mauritania upwelling zone (EUMELI program). Deep-Sea Res. I, *48,* 2251–2282.

Brock, T. D. 1981. Calculating solar radiation for ecological studies. Ecol. Model., *14,* 1–19.

Brown, P. N., G. D. Byrne and A. C. Hindmarsh. 1989. VODE: A Variable Coefficient ODE Solver. SIAM J. Sci. Stat. Comput., *10,* 1038–1051.

Carlson, C. A. and H. W. Ducklow. 1995. Dissolved organic carbon in the upper ocean of the central equatorial Pacific Ocean, 1992: Daily and fine-scale vertical variations. Deep-Sea Res. II, *42,* 621–638.

Claustre, H. and J-C. Marty. 1995. Specific phytoplankton biomasses and their relation to primary production in the tropical North Atlantic. Deep-Sea Res. I, *42,* 1475–1493.

Dadou, I., V. Garçon, V. Andersen, G. R. Flierl and C. S. Davis. 1996. Impact of the north equatorial current meandering on a pelagic ecosystem: A modeling approach. J. Mar. Res., *54,* 311–342.

Dadou, I., F. Lamy, C. Rabouille, D. Ruiz-Pino, V. Andersen, M. Bianchi and V. Garçon. 2001. An integrated biological pump model from the euphotic zone to the sediment: 1-D application in the northeast tropical Atlantic. Deep-Sea Res. II, *48,* 2345–2381.

Denman, K. L. and M. A. Peña. 1999. A coupled 1-D biological/physical model of the northeast Subarctic Pacific Ocean with iron limitation. Deep-Sea Res. II, *46,* 2877–2908.

Doney, S. C., D. M. Glover and R. G. Najjar. 1996. A new coupled one-dimensional biological-physical model for the upper ocean: Application to the JGOFS Bermuda Atlantic Time-series Study (BATS) site. Deep-Sea Res. II, *43,* 591–624.

Ducklow, H. W. and R. P. Harris. 1993. Introduction to the JGOFS North Atlantic Bloom Experiment. Deep-Sea Res. II, *40,* 1–8.

Evans, G. T. 1999. The role of local models and data sets in the Joint Global Ocean Flux Study. Deep-Sea Res. I, *46,* 1369–1389.

—— 2003. Defining misfit between biogeochemical models and data sets. J. Mar. Sys., *40–41,* 49–54.

Evans, G. T. and V. Garçon. 1997. One-dimensional models of water column biogeochemistry. IGBP, JGOFS Report 23, JGOFS Bergen, Norway, 85 pp.

Evans, G. T. and J. S. Parslow. 1985. A model of annual plankton cycles. Biol. Oceanogr., *3,* 327–347.

Geider, R. J., H. L. MacIntyre and T. M. Kana. 1996. A dynamical model of photoadaptation in phytoplankton. Limnol. Oceanogr., *41,* 1–15.

—— 1997. Dynamic model of phytoplankton growth and acclimation: response of the balanced growth rate and the chlorophyll *a*:carbon ratio to light, nutrient-limitation and temperature. Mar. Ecol. Prog. Ser., *148,* 187–200.

Gregg, M. C. 1987. Diapycnal mixing in the thermocline: a review. J. Geophys. Res., *92,* 5249–5286.

Knauer, G. and V. Asper. 1989. Sediment trap technology and sampling. Report of the U.S. GOFS Working Group on Sediment Trap Technology and Sampling, University of Mississippi, 14–18 November 1988, *in* U.S. GOFS Plan. Rep. 10, Woods Hole Oceanographical Institution, Woods Hole, MA, 94 pp.

Kriest, I. 1999. The influence of phytoplankton aggregation on sedimentation—A model study. Ber. Institut für Meerskunde 306—Christian-Albrechts—Universität zur Kiel, 136 pp.

Kriest, I. and G. T. Evans. 1999. Representing phytoplankton aggregates in biogeochemical models. Deep-Sea Res. I, *46,* 1841–1859.

—— 2000. A vertical resolved model for phytoplankton aggregation. Proc. Indian Acad. Sci. (Earth Planet Sci.), *109,* 453–469.

Ledwell, J. R., A. J. Watson and S. L. Clifford. 1998. Mixing of a tracer in the pycnocline. J. Geophys. Res., *103*(C10), 21,499–21,529.

Ledwell, J. R., A. J. Wilson and C. S. Low. 1993. Evidence for slow mixing across the pycnocline from an open-ocean tracer release experiment. Nature, *364,* 701–703.

Lewis, M. R., W. G. Harrison, N. S. Oakey, D. Herbert and T. Platt. 1996. Vertical nitrate fluxes in the oligotrophic ocean. Science, *234,* 870–873.

Morel, A. 1996. An ocean flux study in eutrophic, mesotrophic and oligotrophic situations: the EUMELI program. Deep-Sea Res. I, *43,* 1185–1190.

—— 2000. Process studies in eutrophic, mesotrophic and oligotrophic ocean regimes within the tropical northeast Atlantic, *in* The Changing Ocean Carbon Cycle, IGBP book series, R. B. Hanson, H. W. Ducklow and J. G. Field, eds., Cambridge University Press, NY, 338–374.

Morel, A., D. Antoine, M. Babin and Y. Dandonneau. 1996. Measured and modeled primary production in the northeast Atlantic (EUMELI JGOFS program): the impact of natural variations in photosynthetic parameters on model predictive skill. Deep-Sea Res. I, *43,* 1273–1304.

Oschlies, A. and V. Garçon. 1998. Eddy induced enhancement of primary production in a coupled ecosystem-circulation model of the North Atlantic. Nature, *394,* 266–269.

—— 1999. An eddy-permitting coupled physical-biological model in the North Atlantic: 1, Advection numerics and mixed layer physics. Global Biogeochem. Cycles, *13,* 135–160.

Oschlies, A., W. Koeve and V. Garçon. 2000. An eddy-permitting coupled physical-biological model of the North Atlantic: 2, Ecosystem dynamics and comparison with satellite and JGOFS local studies data. Global Biogeochem. Cycles, *14,* 499–523.

Passow, U. and R. Peinert. 1993. The role of plankton in particle flux: two case studies from the North Atlantic. Deep-Sea Res. II, *40,* 573–586.

Press, W. H., S. A. Teukolsky, W. T. Vetterling and B. P. Flannery. 1992. Numerical Recipes in C, 2nd ed., Cambridge University Press, Cambridge, 994 pp.

Pujo-Pay, M. and P. Raimbault. 1994. Observations chimiques et biomasse dans l'océan Atlantique tropical Nord; campagnes EUMELI. Résultats des mesures. Rapport Centre Océanologique de Marseille, France, 65 pp.

Reed, R. K. 1976. On estimating insolation over the ocean. J. Phys. Oceanogr., *7,* 482–485.

Schwefel, H.-P. 1995. Evolution and Optimum Seeking, Wiley, NY, 444 pp.

SCOR. 1992. Joint Global Ocean Flux Study: Implementation Plan. Scientific Committee on Ocean Research. JGOFS Report No. 9.

Steinberg, D. K., C. A. Carlson, N. R. Bates, R. J. Johnson, A. F. Michaels and A. H. Knap. 2001. Overview of the US JGOFS Bermuda Atlantic Time Series Study (BATS): a decade-scale look at ocean biology and biogeochemistry. Deep Sea Res. II, *48,* 1405–1448.

Received: *30 July, 2003;* revised: *6 May, 2004.*